

Channelrhodopsin-2, a directly light-gated cation-selective membrane channel

Georg Nagel^{†‡}, Tanjef Szellas^{†§}, Wolfram Huhn[†], Suneel Kateriya[†], Nona Adeishvili[†], Peter Berthold[†], Doris Ollig[†], Peter Hegemann[†], and Ernst Bamberg^{†||}

[†]Max-Planck-Institut für Biophysik, Marie-Curie-Strasse 15, 60439 Frankfurt, Germany; [†]Institut für Biochemie, Universität Regensburg; Universitätsstrasse 31, 93040 Regensburg, Germany; and ^{||}Institut für Biophysikalische Chemie, Johann Wolfgang Goethe-Universität, Biozentrum, D-60439 Frankfurt, Germany

Communicated by Walther Stoeckenius, University of California, San Francisco, CA, September 25, 2003 (received for review April 28, 2003)

Microbial-type rhodopsins are found in archaea, prokaryotes, and eukaryotes. Some of them represent membrane ion transport proteins such as bacteriorhodopsin, a light-driven proton pump, or channelrhodopsin-1 (ChR1), a recently identified light-gated proton channel from the green alga *Chlamydomonas reinhardtii*. ChR1 and ChR2, a related microbial-type rhodopsin from *C. reinhardtii*, were shown to be involved in generation of photocurrents of this green alga. We demonstrate by functional expression, both in oocytes of *Xenopus laevis* and mammalian cells, that ChR2 is a directly light-switched cation-selective ion channel. This channel opens rapidly after absorption of a photon to generate a large permeability for monovalent and divalent cations. ChR2 desensitizes in continuous light to a smaller steady-state conductance. Recovery from desensitization is accelerated by extracellular H⁺ and negative membrane potential, whereas closing of the ChR2 ion channel is decelerated by intracellular H⁺. ChR2 is expressed mainly in *C. reinhardtii* under low-light conditions, suggesting involvement in photoreception in dark-adapted cells. The predicted seven-transmembrane α helices of ChR2 are characteristic for G protein-coupled receptors but reflect a different motif for a cation-selective ion channel. Finally, we demonstrate that ChR2 may be used to depolarize small or large cells, simply by illumination.

voltage clamp | patch clamp | light sensitive | *Chlamydomonas reinhardtii* | *Xenopus laevis* oocyte

Photoreception in animals evolved differently in vertebrates and invertebrates although both use as primary photoreceptor rhodopsin, a seven-transmembrane (7-TM) helix protein with covalently linked retinal. In vertebrates, light-activated rhodopsin initiates a G protein-coupled enzyme cascade that ends in the hydrolysis of cGMP and the closure of the cGMP-regulated cation channels, thus hyperpolarizing the plasma membrane (1–3). Invertebrates also use a rhodopsin-based G protein-coupled signaling cascade, which, however, results in activation of transient receptor potential (TRP)/TRP-like (TRPL)-channels and a depolarization of the membrane potential (4, 5). Microbial-type rhodopsins are also 7-TM retinal proteins but show no sequence homology to animal rhodopsins. The prototype microbial-type rhodopsin is the light-driven proton pump bacteriorhodopsin (BR) (6), a structurally and functionally well understood model system for active transmembrane ion transport (7, 8). Other microbial rhodopsins are light-driven chloride pumps or light sensors, the latter enabling phototaxis by coupling to specific transducers (9–11).

Recently, microbial-type rhodopsins were also found in fungi (12) and algae (13), and it has been known since 1991 that phototaxis and photophobic responses in the green alga *Chlamydomonas reinhardtii* are mediated by rhodopsins with a microbial-type *all-trans* retinal chromophore (14–16). As shown for the green algae *Haematococcus pluvialis* (17), *C. reinhardtii* (18), and *Volvox carteri* (19), the photoreceptor currents are confined to the pigmented eyespot region. Although the ion dependence of the photoreceptor currents in these algae is different, it has been proposed for all three species on the basis of stimulus-response

curves that they comprise a high-intensity and a low-intensity photoreceptor system with one or more rhodopsin species (19–21). For *C. reinhardtii* it was shown that at high flash energies the delay between flash and beginning of the photocurrent is <50 μ s, which led to the suggestion that the photoreceptor and the channel form a protein complex (22) or are even one and the same protein (21). At low flash intensities the photoreceptor current is delayed by several milliseconds, suggesting that the low-intensity photoreceptor system involves a signal amplification system that activates the conductance indirectly (19). Under physiological conditions photoreceptor currents are carried mainly by Ca²⁺, but K⁺ is also conducted when the driving force is enhanced at high extracellular K⁺ (23). When the eyespot region is exposed to low pH a second (H⁺-carried) photoreceptor current component appears (21).

Searching in a *C. reinhardtii* genome database has revealed two cDNA sequences encoding apoproteins with some homology to microbial opsins, channelopsin-1 (Chop1) and channelopsin-2 (Chop2) (24) [originally named chlamyopsins: Cop3 and Cop4 (13), also termed CSOA and CSOB (25) or Acop-1 and Acop-2 (26), respectively] (Fig. 1a and Supporting Text, which is published as supporting information on the PNAS web site). We have recently shown that expression of Chop1 in oocytes of *Xenopus laevis* produces a light-gated conductance that is highly selective for protons, and we suggested that channelrhodopsin-1 (ChR1 = Chop1 + retinal) is the photoreceptor system that mediates the H⁺-carried photoreceptor current (24). Sineshchekov and colleagues (25) generated transformants in which the ratio of Chop1 and its homolog Chop2 was changed by an antisense approach. In an electrical cell population assay that monitors the differential response of cells facing the light versus cells facing away from the light, the authors demonstrated that both ChR1 and ChR2 contribute to the photoreceptor currents (25). Because in ChR1-deprived cells photocurrents at high flash intensities were reduced, whereas in ChR2-deprived cells photocurrents at low flash energies were reduced, the authors concluded that ChR1 mediates the high-intensity response, whereas ChR2 is responsible for low-intensity photocurrents (25). The mechanism for how ChR1 and ChR2 contribute to the photocurrents and to what extent to phobic responses and phototaxis could not be resolved. Generation of photocurrent attributed to ChR2 was described as slow and, in analogy to phototaxis in archaea, coupling of a ChR to its specific transducer was proposed, although the possibility that ChR1 might be an ion channel by itself was taken into account (25). Takahashi and colleagues (26) generated antibodies against Chop1 and

Abbreviations: 7-TM, seven-transmembrane; BR, bacteriorhodopsin; Chop, channelopsin; ChR, channelrhodopsin; NMG, N-methyl-D-glucamine; pH_i, intracellular pH; pH_o, extracellular pH.

[†]To whom correspondence should be addressed. E-mail: georg.nagel@mpibp-frankfurt.mpg.de.

[§]Present address: Abteilung Neuro-und Sinnesphysiologie, Physiologisches Institut, Universität Göttingen, Humboldtallee 23, 37073 Göttingen, Germany.

© 2003 by The National Academy of Sciences of the USA

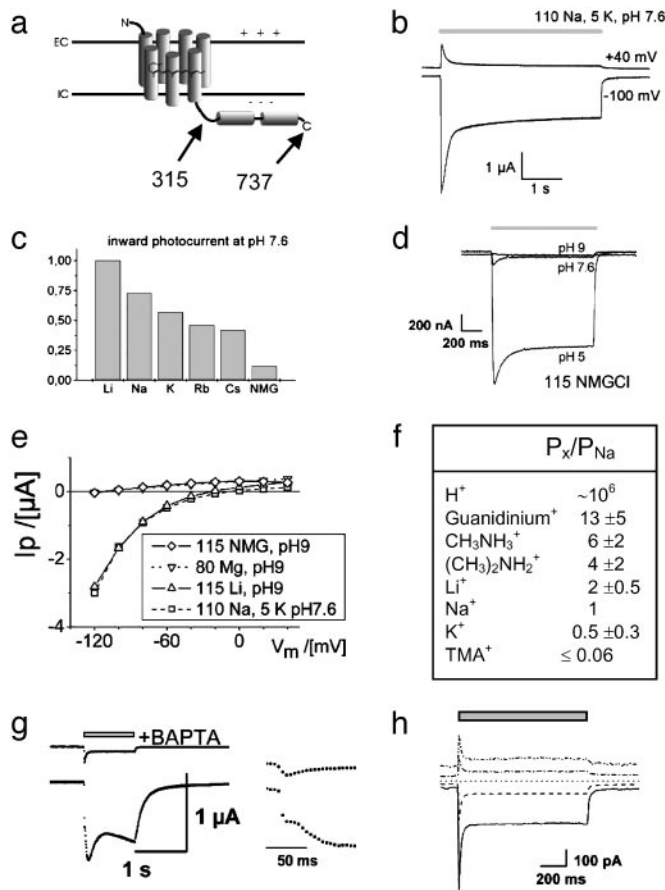


Fig. 1. Ion dependence of light-activated conductance mediated by ChR2-315. Photocurrents of full-length ChR2-737 were indistinguishable. (a) Scheme of the predicted structure of ChR2-737 and ChR2-315. (b) Two-electrode voltage-clamp records from oocytes, expressing ChR2-315, in Ringer's solution (110 mM NaCl, 5 mM KCl, 2 mM CaCl₂, 1 mM MgCl₂, pH 7.6). Illumination with blue (450 ± 25 nm) light is indicated by the gray bar. Currents are typical of those in 23 other experiments. (c) Normalized inward photocurrents at -100 mV, pH 7.6, for 115 mM salt solutions of: LiCl, NaCl, KCl, RbCl, CsCl, and NMG-Cl, measured in the same oocyte. Currents are typical of those in four other experiments. (d) Photocurrents at -100 mV, from the same oocyte, in 115 mM NMG-Cl, at pH 9, pH 7.6, or pH 5. Currents are typical of those in three other experiments. (e) Current–voltage relationship of stationary photocurrents for one representative oocyte (from top to bottom): 115 mM NMG-Cl, pH 9; 80 mM MgCl₂, pH 9 (current–voltage like for NMG, pH 9); 115 mM LiCl, pH 9; 110 mM NaCl, 5 mM KCl, pH 7.6. Currents are typical of those in three other oocytes. (f) Permeability ratios for different monovalent cations, as derived from changes of reversal potentials (31) of photocurrents when replacing Na⁺ by the cation X⁺. Solutions used were: 115 mM XCl, 2 mM BaCl₂, 1 mM MgCl₂, pH 9. The permeability ratio for H⁺ was estimated by the Goldmann–Hodgkin–Katz equation (31) from the photocurrent reversal potential for 115 mM NMG-Cl at pH 9, assuming cytoplasmic ≈ 100 K⁺ and a pH of 7.3. n = 3. (g) Photocurrent in 80 mM CaCl₂, pH 9 at -100 mV (Lower and Inset, higher time resolution). Afterward, the oocyte was injected with 1,2-bis(2-aminophenoxy)ethane-N,N,N',N'-tetraacetate (BAPTA) (as K-salt) to a final concentration of 10 mM, and photocurrent was determined again (Upper and Inset). Currents are typical of those in four other experiments. (h) Photocurrents of a HEK293 cell, transiently expressing ChR2-315. Photocurrents were determined at -100 , -50 , 0 , $+50$, and $+100$ mV. Pipette solution used was 140 mM NaCl, 5 mM EGTA, 2 mM MgCl₂, 10 mM Hepes, pH 7.4. Bath solution used was 140 mM NaCl, 2 mM MgCl₂, 1 mM CaCl₂, 10 mM Hepes, pH 7.4. Currents are typical of those in more than nine other experiments on HEK293 and more than five in BHK cells.

Chop2. They were not able to localize the proteins within the total membrane fraction but detected Chop1 as a 66-kDa protein in enriched eyespot membranes.

Up to now, heterologous expression of ChR2 had not reported, and its primary mode of action remained obscure. We

aimed to express Chop2 in *Xenopus* oocytes and mammalian cells in the hope of obtaining a functional rhodopsin (ChR2) that might reveal its primary function and possibly allow to determine its action spectrum. We were guided by the belief that a function that is observed after heterologous expression in three different animal cells will also be present in the alga, even if in the host system coupling to other proteins of the algal sensory transduction pathway might be missing.

Materials and Methods

A full-length (*chop2-737*) and a C terminally truncated *chop2* variant (*chop2-315*) were produced from a full-length cDNA template (GenBank accession no. AF461397) as described for *chop1* (24). *chop2-315* was additionally subcloned into pBK-CMV and expressed in HEK293 or BHK cells by transient transfection. Mammalian cells were examined with the whole-cell patch-clamp technique (27). For further details see *Supporting Text*.

Results

Expression of ChR2 in Oocytes Yields a Light-Sensitive Cation Conductance. We expressed Chop2 in oocytes of *X. laevis*, in the presence of *all-trans* retinal, to test whether a functional rhodopsin (with covalently linked retinal: ChR2) may be obtained. A full-length ChR2 or a ChR2 fragment comprising only amino acids 1–315 were tested (Fig. 1a and Fig. 5, which is published as supporting information on the PNAS web site). Large light-activated currents were observed with both constructs, in standard oocyte Ringer's solution (Fig. 1b). These photocurrents are completely absent in noninjected oocytes, as reported in previous studies on other rhodopsins, expressed in oocytes under similar conditions (9, 24, 28, 29). In continuous light, the photocurrent decays to a steady-state level, i.e., desensitizes (Fig. 1b). Size and direction of the photocurrent varied with the membrane potential, indicating that light triggers a passive ion conductance of ChR2. The cation conductance of ChR2 is confined to the hypothetical 7-TM helices, as identical photocurrents and very similar current–voltage relationships were obtained with ChR2-737 or ChR2-315, allowing the conclusion that amino acids 316–737 do not contribute to the ion conductance.

In contrast to the proton-selective ion channel ChR1, ChR2 photocurrents greatly varied in solutions containing different cations (Fig. 1c), suggesting that several cations may permeate ChR2. That anions are not contributing to photocurrents was proved by replacing extracellular chloride with aspartate, which changed neither the magnitude nor the reversal potential of photocurrents (data not shown, but see current–voltage for 115 mM NMG-Cl or 80 mM MgCl₂ in Fig. 1e). The dependence of photocurrents on different salt solutions shows a strong inverse relationship with the atomic radius of the cation (Fig. 1c). The small inward photocurrent in presence of the large monovalent cation *N*-methyl-D-glucamine (NMG⁺) at pH 7.6 might indicate that ChR2 is permeable for NMG⁺. However, as the inward photocurrent completely vanishes at pH 9 in NMG-Cl, whereas it remains for LiCl pH 9, we conclude that the inward photocurrent in the presence of NMG-Cl is a proton flux, which becomes highly obvious at pH 5 (Fig. 1d).

To get an estimate of the permeability for different cations, we measured photocurrent–voltage relationships and the reversal potential for different cations at pH 9. These experiments revealed that neither NMG⁺ nor Mg²⁺ are conducted to a measurable degree (Fig. 1e). A graded-size series of different organic cations revealed permeability for methyl-ammonium, di-methyl-ammonium, and even for tetra-methyl-ammonium (Fig. 1f), whereas tetra-ethyl-ammonium does not measurably permeate ChR2. The series indicates that the effective ChR2 pore must be larger than that of the voltage-activated Na⁺

channel, which cannot be passed by methyl-ammonium (30, 31). Whereas in most voltage-activated Na^+ channels the permeability for guanidinium is $\approx 13\%$ of that for Na^+ (30, 31) we found a large light-gated permeability of ChR2 for guanidinium (Fig. 1f). This fact, together with the permeability for methylated ammonium compounds, implies an effective pore size, exceeding that of the voltage-activated Na^+ channel. From the observation that the conductance for monovalent metal ions decreases with increasing atomic radius it may be concluded that the cations permeate the selectivity filter (31) in a mostly dehydrated state (i.e., without a complete inner water shell).

In addition to monovalent cations, ChR2 is permeable for divalent cations. In solutions containing 80 mM Ca^{2+} , activation of ChR2 triggers a large current (Fig. 1g Lower) with a biphasic rise time (Fig. 1g Inset). This current is best explained by a fast light-activated Ca^{2+} entry into the cytosol, leading to a slower activation of the oocyte-endogenous Ca^{2+} -sensitive chloride channels (32, 33). This hypothesis was confirmed by the strong reduction of this photocurrent in presence of the inhibitor of Ca^{2+} -sensitive chloride channels, niflumic acid, or by reduction of cytosolic free $[\text{Ca}^{2+}]$ with the fast Ca^{2+} -chelator 1,2-bis(2-aminophenoxy)ethane-*N,N,N',N'*-tetraacetate (BAPTA). BAPTA injection into oocytes led to suppression of the previously observed, more slowly rising, light-activated current (Fig. 1g Upper). The remaining photocurrent then reflects the true size of the Ca^{2+} conductance. The relative permeability of ChR2, as estimated from inward current at -100 mV and 80 mM divalent cation, follows the sequence $\text{Ca}^{2+} > \text{Sr}^{2+} > \text{Ba}^{2+} \gg \text{Zn}^{2+}, \text{Mg}^{2+} (\approx 0)$ and is, with the exception of Mg^{2+} , again inversely related to atomic radius. The lack of permeability to Mg^{2+} is most likely caused by the strong hydration of Mg^{2+} (31, 34), in accordance with the suggested permeation of largely dehydrated cations.

Expression of ChR2 in Mammalian Cells. To demonstrate that the properties of the ChR2 conductance are quite independent of the host system, ChR2-315 was expressed in HEK293 and BHK cells. In these cells ChR2 also produced a light-switched large passive cation conductance that upon illumination of the cell rapidly activates and then desensitizes to a stationary level (Fig. 1h), very similarly as it does in *Xenopus* oocytes. These whole-cell patch-clamp experiments specifically supported the notion that the light-induced conductance is purely passive, as the reversal potential for symmetrical ion concentrations was at 0 mV (Fig. 1h). These experiments also revealed that the light-activated conductance for Na^+ is inward rectifying.

Desensitization of ChR2 Is Influenced by Membrane Potential and pH. As seen from Fig. 1b, the ChR2 photocurrent decays to a stationary level, which might be caused by a switch to a different conducting state or inactivation of a fraction of ChR2 molecules. After equilibration in the light, the stationary current is stable. However, the response to a second pulse, given after a short dark phase, includes a smaller transient current component than the first response. The recovery of the peak current depends on the membrane potential, i.e., recovery is faster at negative than at positive voltage (Fig. 2 a–c). The recovery from inactivation also depends on extracellular pH (pH_o): it is slower at higher pH_o (Fig. 2d) than at low pH_o (Fig. 2e). A H^+ pulse, given during the dark period, accelerates recovery of ChR2 from the desensitized state (Fig. 2f). This result suggests that the recovery from the inactive state is linked to protonation of one or more amino acids from the extracellular side. Mutation of Glu-123, an amino acid predicted to be exposed to the extracellular side (because of its position analog to Asp-85 in BR, see Fig. 5), to Asp resulted in a similar photocurrent, with an increased ratio of transient to steady-state photocurrent (Fig. 2g). Mutation of Glu-123 to Gln abolished the peak photocurrent completely but also resulted in

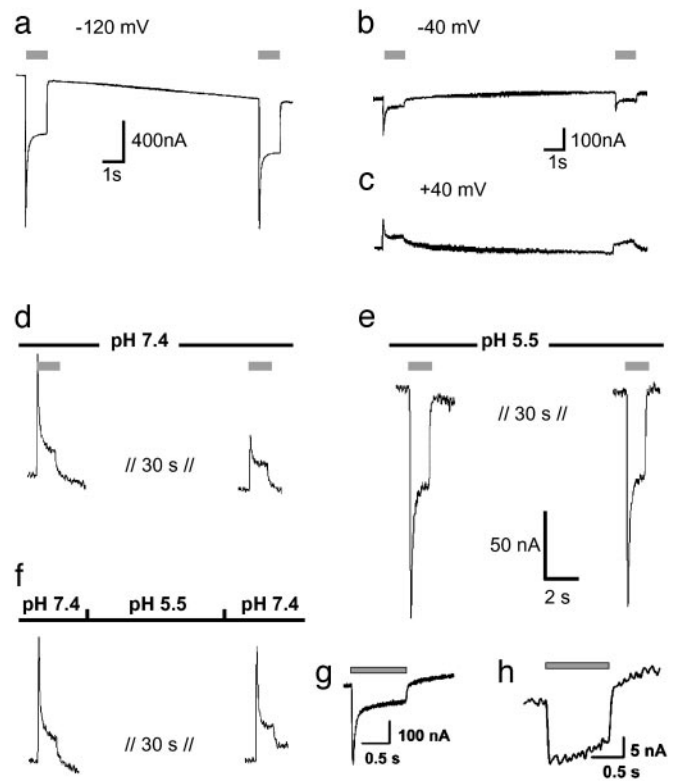


Fig. 2. Recovery from desensitization of photocurrents is voltage and pH_o dependent. Currents are typical of those in three other experiments. (a–c) Two light pulses with a dark phase of 10 s, $\text{pH}_o = 7.6$, the same oocyte at -120 mV (a), -40 mV (b), and $+40\text{ mV}$ (c). (d) Another oocyte at $\text{pH}_o = 7.4$, $+20\text{ mV}$, 32 s dark between light pulses. (e) The same oocyte, $\text{pH}_o = 5.5$. (f) The same oocyte as in d and e, $\text{pH}_o = 7.4$ during light flash, but $\text{pH}_o = 5.5$ for 20 s during the dark phase. Light pulses are indicated by gray bars. (g) Photocurrent of ChR2-315-E123D at -100 mV , $\text{pH} = 7.6$. (h) Photocurrent of ChR2-315-E123Q at -100 mV , $\text{pH} = 7.6$.

a strong reduction of the stationary photocurrent (Fig. 2h). We suggest that E123 changes the protonation state in the light, thus mediating desensitization of ChR2.

Photocurrents Observed in Excised Patches of Plasma Membrane. The influence of the cytoplasm on photocurrents of ChR2 was studied under cell-free conditions in excised giant inside-out membrane patches, where the cytoplasmic solution was controlled reliably and readily (35–37). To simplify the analysis, we studied H^+ -carried photocurrents with bath solutions of different intracellular pH (pH_i). The photocurrent again declined toward a stable steady state in this cell-free system, and the transient component was reduced upon a second stimulation (Fig. 3a), showing that inactivation of ChR2 is an intrinsic property of the protein and not caused by any kind of modification by soluble oocyte components.

ChR2 Itself Is the Cation Channel. The patch experiments prove that ChR2 itself mediates the light-gated passive cation conductance and that it is not triggering the gating of a channel via a soluble messenger, as rhodopsin does in animal photoreceptor systems (1–5). To analyze more precisely the rise and decay of the conducting state, ChR2 was stimulated with two subsequent laser flashes of only 10-ns duration (Fig. 3b). The rise of ChR2-induced photocurrents is extremely fast, with no visible delay and a rise time of $\approx 200\text{ }\mu\text{s}$ or faster (Fig. 3c). Such a fast opening is found only in ion channels that are activated either by voltage changes or ligand binding, but until now, never in ion

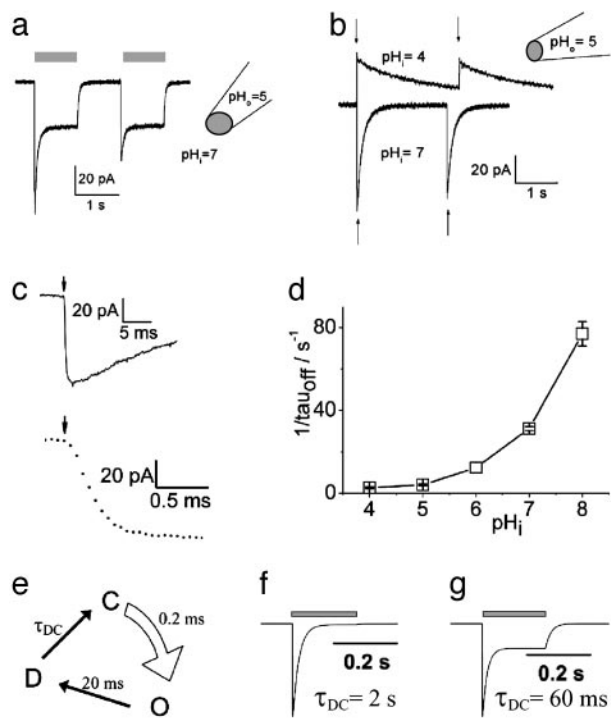


Fig. 3. Activation of ChR2 photocurrents in excised inside-out giant membrane patches from *Xenopus* oocytes. This configuration allows a rapid concentration change (≈ 100 ms; ref. 43) at the cytoplasmic side by changing the superfusing bath solution. (a) Activation of inward photocurrents by light pulses of 442 nm (gray bars). Pipette solution used was 115 mM NMG-Cl, pH 5; bath (cytoplasmic solution) used was 115 mM NMG-Cl, pH 7. Currents typical of those in nine other experiments are shown. (b) Activation of photocurrents by two laser flashes of 10-ns duration (arrows), 440 nm. Pipette solution used was 115 mM NMG-Cl, pH 5; bath solution used was 115 mM NMG-Cl, pH 7 or 115 mM NMG-Cl, pH 4, as indicated. Currents typical of those in three other experiments are shown. (c) Higher time resolution of first photocurrent, shown in b, pH_i = 7. (d) Dependence of closing rate on pH_i ($n = 4 - 7$). (e) Simple three-state model of ChR2 photocycle. Light, curved arrow indicates light-activated step from ChR2-ground state (C) to open state (O). Straight arrows indicate dark reactions, to the closed desensitized state (D) and back to the ground state (C). For further details see text. (f) Simulated photocurrent with $\tau_{DC} = 2$ s and other time constants as in the model depicted in e. (g) Simulated photocurrent with $\tau_{DC} = 60$ ms and other time constants as in e.

channels that are activated via a chemical signal transduction system. This rapid activation and the complete replacement of the intracellular medium support the notion that activation is independent of a diffusible cytoplasmic transmitter.

pH_i Determines the Speed of Channel Closing. Giant-patch experiments have also shown that the decay of the photocurrent upon light-off strongly depends on the pH_i (Fig. 3 b and d), whereas it is virtually independent of pH_o, as observed in experiments with whole oocytes. The slower photocurrent decay at high intracellular H⁺ concentrations suggests that proton release to the cytoplasmic side precedes closing. The large photocurrent and the slow kinetics are incompatible with a mechanism, where transport and photocycle are intimately connected. However, they are well in agreement with a mechanism where an intermediate of the photocycle allows passive ion transport.

Analysis of Photocurrents and Modeling of the Photocycle. Although ChR2 was so far heterologously expressed only in tiny amounts and no protein is at hand for spectroscopic studies, our recorded photocurrents allow modeling of a simple photocycle. As found for any rhodopsin so far investigated, it may be assumed that an

ultrafast (<1 ns) light-activated step leads to an excited state of ChR2 (C*). This will be followed by slower dark reactions to an open state (O), a closed, desensitized state (D), and a closed ground state (C). From the fast opening of ChR2 (Fig. 3c) we can assign a time constant of <1 ms to the steps leading to the open state (C → C* → O), whereas closing to the desensitized state (D) proceeds with 10–400 ms, depending on pH_i (Fig. 3d).

As opening (C → C* → O) is so fast, the four-state model (C → C* → O → D → C) can be further reduced to a three-state model (C → O → D → C) (38) [see Fig. 3e, e.g., with a time constant of 0.2 ms for light-activated opening (C → O) as obtained from Fig. 3c, of 20 ms for closing (O → D) at pH_i = 7.3 as obtained from Fig. 3d, and of 2 s for recovery from desensitization (D → C) as obtained from Fig. 2a]. When using these time constants, then the model predicts a much smaller stationary photocurrent (Fig. 3f) than experimentally observed (Fig. 3a). The photocurrent in Fig. 3a, however, may be obtained by this model, if assuming a faster recovery from desensitization (D → C), e.g., with a time constant of 60 ms (see Fig. 3g). The discrepancy with the observed recovery in the dark (see Fig. 2) might indicate absorption of two photons during the photocycle, i.e., a light-activated D → C transition with an effective time constant of 60 ms. The notion that intermediates of the photocycle show photoreactions, resulting in a two-photon cycle, is not new for retinal proteins, e.g., halorhodopsin (39) or proteorhodopsin (40). Alternatively, a four-state photocycle with two closed states, two open states (a larger conductance for the open state of the first photocycle and a smaller for the following photocycles, i.e., the desensitized state is comprised of a closed and an open state), and a slow transition in the dark to the initial closed state, could also explain the shape of the observed photocurrent. As no experimental data exist yet to decide between these models, further experiments will have to show more details of the photocycle. Once enough ChR2 protein is available, spectroscopic measurements on ChR2 will certainly improve photocycle models and probably add new intermediates. The presented electrical data, however, already set a lower limit on the turnover time for the photocycle, e.g., >60 ms at a pH_i of 7.3.

Light Dependence of ChR2 Action and Expression in *Chlamydomonas*. In oocytes, the action spectrum of the ChR2 photocurrents is a typical rhodopsin spectrum with the maximum at ≈ 460 nm (Fig. 4a). The spectrum almost exactly matches the Dartnall rhodopsin nomogram (41) but the spectrum is blue-shifted by 40 nm relative to the action spectrum for ChR1 photocurrents (Fig. 4a). The presence of Chop1 and Chop2 was examined in *Chlamydomonas* membrane fractions by using antibodies against the C-terminal hydrophilic end of both proteins (Fig. 4 b and c). Chop2 appeared as a 70-kDa species, whereas Chop1 is seen as a triplet with molecular masses between 60 and 66 kDa. Both proteins are most abundant, when the cells were grown under low-light conditions or in darkness. Both are degraded under high light conditions (Fig. 4) and almost completely disappear when the cell culture is approaching the stationary phase. ChR2 is degraded more rapidly than ChR1.

We have measured an action spectrum for flash-induced photoreceptor currents in young *C. reinhardtii* cells at pH 9, where the proton conducting ChR1 is expected to be of low efficiency. The pH 9 spectrum shows a maximum ≈ 485 nm, which is blue-shifted with respect to all earlier photocurrent spectra, recorded from untransformed single cells or cell populations (18, 20, 21), suggesting that ChR2 is contributing to photoreceptor currents at high pH.

ChR2 May Be Used to Depolarize Animal Cells. We reasoned that ChR2 should be able to significantly depolarize a *Chlamydomonas* cell and, second, that heterologous expression of ChR2

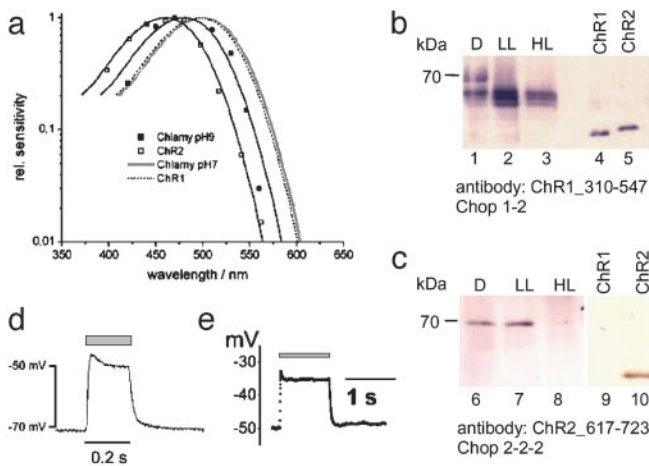


Fig. 4. Action spectra of ChR2 and ChR1, antibody staining of *C. reinhardtii* membrane fractions, and ChR2-induced membrane depolarization. (a) Normalized action spectra for the ChR2-mediated inward current from oocytes at $\text{pH}_0 = 7.6$ and -100 mV (\square , $n = 3$) and for the high-light saturating photoreceptor current from *C. reinhardtii* strain CW2 at pH 9 (\blacksquare). *C. reinhardtii* cells were grown at low light (0.5 W m^{-2}) for 3 days. Photocurrents were recorded directly from the eye spot with NMG-Hepes, 2 mM Ca^{2+} , and 2 mM K^+ in the pipette (21). Solid lines show the standard rhodopsin spectrum [Dartnall spectrum (41)], fitted to the data points. Spectra of the ChR1 photocurrent, measured in oocytes (24), and of photoreceptor currents, recorded from *C. reinhardtii* at pH 7 (21), are plotted for comparison. (b and c) *C. reinhardtii* cells were grown in darkness (D), low light conditions (LL; 0.5 W m^{-2}) and high light conditions (HL; 10 W m^{-2}). Membrane fractions were collected and analyzed by protein immunoblotting. Chop1₃₁₀₋₅₄₆ antiserum (1:1,000 dilution) was raised against a Chop1-310-546 fragment in rabbits. (b) It identified Chop1 and Chop2. (c) Chop2₆₁₇₋₇₂₃ antiserum (raised against a Chop2-617-723-fragment) is specific for Chop2. Binding was detected by using an alkaline phosphatase-coupled second antibody. Chop1 and Chop2 fragments expressed in *Escherichia coli* (lanes 4, 5, 9, and 10) are blotted for comparison. (d and e) Depolarization of ChR2-expressing cells by blue light, as indicated by gray bar. Voltages typical of those in four other experiments are shown. (d) An oocyte, expressing ChR2-315, in Ringer's solution ($110 \text{ mM NaCl}/5 \text{ mM KCl}/2 \text{ mM CaCl}_2/1 \text{ mM MgCl}_2$, pH 7.6). (e) A HEK293 cell, transiently expressing ChR2-315. Pipette solution used was $140 \text{ mM KCl}, 5 \text{ mM EGTA}, 2 \text{ mM MgCl}_2, 10 \text{ mM Hepes}$, pH 7.4. Bath solution used was $140 \text{ mM NaCl}, 2 \text{ mM MgCl}_2, 1 \text{ mM CaCl}_2, 10 \text{ mM Hepes}$, pH 7.4.

should become a useful tool to manipulate intracellular Ca^{2+} concentration (Fig. 1g) or membrane potential, especially in mammalian cells. Current-clamp experiments with ChR2-expressing oocytes (Fig. 4d) or HEK293 cells of similar diameter as a *Chlamydomonas* cell (Fig. 4e) to test this promise clearly demonstrated a fast light-induced depolarization by tens of mV when the cells were illuminated with blue light.

Discussion

This study addressed the question of what the molecular function of the second microbial-type retinal protein (rhodopsin), ChR2, from the alga *C. reinhardtii* might be. The involvement of ChR2 in the generation of photocurrents in *C. reinhardtii* was shown in a recent study (25). Sineshchekov *et al.* (25) named this rhodopsin CSRB (*Chlamydomonas* sensory rhodopsin B), as its molecular function was revealed indirectly (by suppression of endogenous expression), and postulated, in analogy to the archaeal sensory rhodopsins, coupling to a transducer.

From the large photocurrents in Chop2-expressing *Xenopus* oocytes, or the mammalian (HEK293 and BHK) cells, we can conclude that ChR2 from *C. reinhardtii* is functionally expressed in our host systems, i.e., amphibian and mammalian cells. The experiments leave little doubt that Chop2 binds retinal to form ChR2 and that ChR2 is a rhodopsin that undergoes a photocycle

with a cation-conducting photocycle intermediate or, in other words, an ion channel with intrinsic light sensor. The channel has a low selectivity among cations but it is not unspecific because it does not conduct anions. From the range of conducted cations it may be concluded that the narrowest pore size or selectivity filter of the channel (31) is wider than that of a voltage-activated Na^+ channel but probably slightly smaller than that of the nicotinic acetylcholine receptor, because tetraethyl ammonium $^+$, Mg^{2+} , and Zn^{2+} were not conducted.

Both ChR1 and ChR2 reveal a 7-TM motif that is well known for other microbial type rhodopsins and for G protein-coupled receptors but new for ion channels. Most ion channels are formed by polymers of subunits or are large proteins with internal repeats (31). A well-known exception is the cystic fibrosis transmembrane conductance regulator, where a single 12-transmembrane protein forms a chloride channel (42). Formation of a cation channel pore by a 7-TM protein, however, was unknown until now. The light-gated proton channel of ChR1 (24) could be understood because it is established for the light-driven ion pump BR that the actively transported proton moves along a hydrogen-bonded network, formed by monomeric BR. For ChR2 we propose that 7-TM helices form a cation channel that must be wide ($\approx 6 \text{ \AA}$ in diameter) to be permeable to methylated ammonium cations. In analogy to other rhodopsins, we suggest that the channel is opened by a conformational change of the protein, after a light-induced isomerization of *all-trans* retinal.

Assuming an expression density of ChR2 in the plasma membrane similar to BR (2×10^9 per oocyte; ref. 28) we can calculate a single channel current for one ChR2 molecule. At -100 mV we obtained typically an inward current of $1 \mu\text{A}$ (photoconductance $\approx 10 \mu\text{S}$), which corresponds to $5 \times 10^{-16} \text{ A}$ per molecule if all ChR2 channels were open at saturating light. Assuming that $\approx 10\%$ of ChR2 are in the open state (see model on photocycle), yields 5 fA (or a single-channel conductance of $\approx 50 \text{ fS}$) for a single-channel event. Although a current step of 5 fA corresponds to a turnover of $\approx 3 \times 10^4$ ions per s, it is still too small to be observed, and single-channel events were not observed.

We have no indication that ChR1 or ChR2 are coupled to any signal-acceptor protein, like a G protein, or to a transducer, like the archaeal sensory rhodopsins I and II to their respective transducers. This notion is corroborated by the finding that the electrical properties of ChR1 and ChR2 are independent of the large hydrophilic half of the protein, C-terminal of the 7-TM region. In *C. reinhardtii*, evidence exists for two separate light-activated conductances for H^+ and Ca^{2+} but the rise times of the Ca^{2+} current and the H^+ current are indistinguishable (21). Therefore, it was impossible to decide whether both currents are directly light-gated or which of the two currents triggers the other. On the basis of the experiments described for expressed ChR1 (24) and ChR2 (above) we propose the following: The high-light photoreceptor current of *C. reinhardtii* is triggered by ChR1 and/or ChR2. The local depolarization or the H^+ influx is then most likely activating a secondary Ca^{2+} conductance, also confined to the eyespot region. This secondary photoreceptor conductance decays faster (21) than the primary current but its molecular origin still has to be identified.

Photocurrent measurements on cell populations with altered ChR1 and ChR2 content have demonstrated that both photoreceptors contribute to photoreceptor currents in *Chlamydomonas* (25). The cellular sensitivity in ChR1-depleted cells was reported to be blue-shifted by $\approx 40 \text{ nm}$ compared with ChR2-depleted cells, and it was suggested that ChR2 absorption is blue-shifted as compared with ChR1. That heterologously expressed ChR2 indeed shows a blue-shifted action spectrum relative to ChR1 was shown by this investigation, therefore confirming the earlier suggestion (25). The previously reported

slow activation of ChR2-attributed photocurrents (25) is, however, in contrast to the very rapid ($<200\ \mu\text{s}$) activation of ChR2 photocurrents.

ChR2 may be a sensory photoreceptor that is preferentially used when the cells are exposed to dim light for longer time periods (several hours). From the fact that ChR2 triggers much larger photocurrents than ChR1 it is immediately obvious that the observed degradation of ChR2 at higher light intensities will protect cells from the detrimental effects of continuously inward flowing cations, especially protons and calcium.

This study revealed an important function for a microbial-type rhodopsin, a directly light-switched cation channel, and demonstrated the likelihood of a mechanism in light signal transduction

as it may be used in *C. reinhardtii*. Additionally, we have shown that expression of ChR2 in oocytes or mammalian cells may be used as a powerful tool to increase cytoplasmic Ca^{2+} concentration or to depolarize the cell membrane, simply by illumination.

We thank Mrs. Saskia Schröder-Lang for preliminary giant-patch data, Ms. Anna Greening for photocurrent reversal potential measurements, and Dr. Klaus Fendler (all at Max-Planck-Institute of Biophysics) for advice on kinetic models. We thank Dr. Richard Henderson (Medical Research Council, Cambridge, U.K.) for helpful comments on an earlier draft of the manuscript. This work was supported by the Deutsche Forschungsgemeinschaft (E.B., P.H., and G.N.).

1. Kaupp, U. B. (1995) *Curr. Opin. Neurobiol.* **5**, 434–442.
2. Okada, T., Ernst, O. P., Palczewski, K. & Hofmann, K. P. (2001) *Trends Biochem. Sci.* **26**, 318–324.
3. Sakmar, T. P., Menon, S. T., Marin, E. P. & Awad, E. S. (2002) *Annu. Rev. Biophys. Biomol. Struct.* **31**, 443–484.
4. Zuker, C. S. (1996) *Proc. Natl. Acad. Sci. USA* **93**, 571–576.
5. Hardie, R. C. & Raghu, P. (2001) *Nature* 186–193.
6. Oesterhelt, D. & Stoeckenius, W. (1971) *Nat. New Biol.* **233**, 149–152.
7. Henderson, R., Baldwin, J. M., Ceska, T. A., Zemlin, F., Beckmann, E. & Downing, K. H. (1990) *J. Mol. Biol.* **213**, 899–929.
8. Lanyi, J. K. & Luecke, H. (2001) *Curr. Opin. Struct. Biol.* **11**, 415–419.
9. Schmies, G., Engelhard, M., Wood, P. G., Nagel, G. & Bamberg, E. (2001) *Proc. Natl. Acad. Sci. USA* **98**, 1555–1559.
10. Spudich, J. L. & Luecke, H. (2002) *Curr. Opin. Struct. Biol.* **12**, 540–546.
11. Gordeliy, V. I., Labahn, J., Moukhametzianov, R., Efremov, R., Granzin, J., Schlesinger, R., Büldt, G., T., S., Scheidig, A. J., Klare, J. P. & Engelhard, M. (2002) *Nature* **419**, 484–487.
12. Bieszke, J. A., Braun, E. L., Bean, L. E., Kang, S., Natvig, D. O. & Borkovich, K. A. (1999) *Proc. Natl. Acad. Sci. USA* **96**, 8034–8039.
13. Hegemann, P., Fuhrmann, M. & Kateriya, S. (2001) *J. Phycol.* **37**, 668–676.
14. Hegemann, P., Gärtner, W. & Uhl, R. (1991) *Biophys. J.* **60**, 1477–1489.
15. Lawson, M. A., Zacks, D. N., Derguini, F., Nakanishi, K. & Spudich, J. L. (1991) *Biophys. J.* **60**, 1490–1498.
16. Takahashi, T., Yoshihara, K., Watanabe, M., Kubota, M., Johnson, R., Derguini, F. & Nakanishi, K. (1991) *Biochem. Biophys. Res. Commun.* **178**, 1273–1279.
17. Litvin, F. F., Sineshchekov, O. A. & Sineshchekov, V. A. (1978) *Nature* **271**, 476–478.
18. Harz, H. & Hegemann, P. (1991) *Nature* **351**, 489–491.
19. Braun, F. J. & Hegemann, P. (1999) *Biophys. J.* **76**, 1668–1678.
20. Sineshchekov, O. A., Govorunova, E. G., Der, A., Keszhelyi, L. & Nultsch, W. (1994) *Biophys. J.* **66**, 2073–2084.
21. Ehlenbeck, S., Gradmann, D., Braun, F.-J. & Hegemann, P. (2002) *Biophys. J.* **82**, 740–751.
22. Harz, H., Nonnengässer, C. & Hegemann, P. (1992) *Philos. Trans. R. Soc. London B* **338**, 39–52.
23. Holland, E. M., Braun, F. J., Nonnengässer, C., Harz, H. & Hegemann, P. (1996) *Biophys. J.* **70**, 924–931.
24. Nagel, G., Ollig, D., Fuhrmann, M., Kateriya, S., Musti, A. M., Bamberg, E. & Hegemann, P. (2002) *Science* **296**, 2395–2398.
25. Sineshchekov, O. A., Jung, K.-H. & Spudich, J. L. (2002) *Proc. Natl. Acad. Sci. USA* **99**, 8689–8694.
26. Suzuki, T., Yamasaki, K., Fujita, S., Oda, K., Iseki, M., Yoshida, K., Watanabe, M., Daiyasu, H., Toh, H., Asamizu, E., et al. (2003) *Biochem. Biophys. Res. Commun.* **301**, 711–717.
27. Hamill, O. P., Marty, A., Neher, E., Sakmann, B. & Sigworth, F. J. (1981) *Pflügers Arch.* **391**, 85–100.
28. Nagel, G., Möckel, B., Büldt, G. & Bamberg, E. (1995) *FEBS Lett.* **377**, 263–266.
29. Nagel, G., Kelety, B., Möckel, B., Büldt, G. & Bamberg, E. (1998) *Biophys. J.* **74**, 403–412.
30. Hille, B. (1971) *J. Gen. Physiol.* **58**, 599–619.
31. Hille, B. (2001) *Ion Channels of Excitable Membranes* (Sinauer, Sunderland, MA).
32. Takahashi, T., Neher, E. & Sakmann, B. (1987) *Proc. Natl. Acad. Sci. USA* **84**, 5063–5067.
33. Stühmer, W. (1992) *Methods Enzymol.* **207**, 319–339.
34. Diebler, H., Eigen, M., Ilgenfritz, G., Maas, G. & Winkler, R. (1969) *Pure Appl. Chem.* **20**, 93–115.
35. Hilgemann, D. W. (1989) *Pflügers Arch.* **415**, 247–249.
36. Hilgemann, D. W. (1990) *Nature* **344**, 242–245.
37. Nagel, G., Hwang, T. C., Nastiuk, K. L., Nairn, A. C. & Gadsby, D. C. (1992) *Nature* **360**, 81–84.
38. Gropp, T., Cornelius, F. & Fendler, K. (1998) *Biochim. Biophys. Acta* **1368**, 184–200.
39. Hegemann, P., Oesterhelt, D. & Bamberg, E. (1985) *Biochim. Biophys. Acta* **819**, 195–205.
40. Friedrich, T., Geibel, S., Kalmbach, R., Chizhov, I., Ataka, K., Heberle, J., Engelhard, M. & Bamberg, E. (2002) *J. Mol. Biol.* **321**, 821–838.
41. Dartnall, H. J. A. (1972) in *Photochemistry of Vision*, ed. Dartnall, H. J. A. (Springer, New York), pp. 122–145.
42. Chen, J. H., Chang, X. B., Aleksandrov, A. A. & Riordan, J. R. (2002) *J. Membr. Biol.* **188**, 55–71.
43. Weinreich, F., Riordan, J. R. & Nagel, G. (1999) *J. Gen. Physiol.* **114**, 55–70.